THE PROGRAM TO LINK THE *HIPPARCOS* REFERENCE FRAME TO AN EXTRAGALACTIC REFERENCE SYSTEM USING THE FINE GUIDANCE SENSORS OF THE *HUBBLE SPACE TELESCOPE*

P. D. HEMENWAY,[1–4] R. L. DUNCOMBE,[2] E. P. BOZYAN,[1,3] A. M. LALICH,[1,2,5] A. N. ARGUE,[6] O. G. FRANZ,[7] B. MCARTHUR,[1] E. NELAN,[1,8] D. TAYLOR,[8] G. WHITE,[9] G. F. BENEDICT,[1] F. CRIFO,[10] L. W. FREDRICK,[11] W. H. JEFFERYS,[12] K. JOHNSTON,[13] J. KOVALEVSKY,[14] J. KRISTIAN,[15,16] M. A. C. PERRYMAN,[17] R. PRESTON,[18] P. J. SHELUS,[1] C. TURON,[10] AND W. VAN ALTENA[19]

Received 1997 June 27; revised 1997 September 2; accepted 1997 September 8

ABSTRACT

The *Hipparcos* Satellite Mission has produced positions, proper motions, and parallaxes of unprecedented accuracy for 118,000 stars. For the positions and proper motions to represent true directions and physical motions in space, they must refer to an accurate realization of a nonrotating (inertial) reference frame. One of the major problems confronting the *Hipparcos* Project was the determination of the relationship of the satellite coordinate system to the best available celestial coordinate system, hopefully at an accuracy approaching the systematic accuracy of the *Hipparcos* satellite itself. In 1978 we recognized the possibility of using the Fine Guidance Sensors of the *Hubble Space Telescope* (*HST*) to measure the *Hipparcos* coordinate offset and its time variation with respect to extragalactic objects, and we undertook that project. The first *HST* observation for the project was made in 1993 April, and the last observation used in the solution was made in 1995 October. The *HST* data consist of accurate angular separations of Extragalactic Objects from *Hipparcos* stars. Ultimately the *HST* solution was incorporated with other techniques to form the final link between *Hipparcos* and the International Celestial Reference System. This link determined the final catalogue system for the published *Hipparcos* data. We describe the problem, the instrumentation of the two space missions, the limitations imposed by the missions on the observations, the reduction and analysis procedures, and the final results with respect to the final *Hipparcos* solution. We determine the relation of the *Hipparcos* coordinate axes with respect to the ICRS coordinate axes from the *HST*, *Hipparcos*, and VLBI data alone. The rms uncertainties are about 2 milliarcseconds for the angular offsets and about 2.5 milliarcseconds/yr for the angular rotations. © *1997 American Astronomical Society.* [S0004-6256(97)03612-1]

1. INTRODUCTION

In 1989 August, the European Astrometry Satellite *HIPPARCOS* was launched. During the course of the next three years, the satellite produced data that resulted in the measurement of the positions, parallaxes, and proper motions of approximately 118,000 stars with accuracies of about one milliarcsecond (mas) and one mas/year. Because the limiting magnitude of the satellite was about 13th, the satellite could not observe quasars directly (except 3C 273, and that with reduced accuracy). The data consist of chords along great circles on the celestial sphere, and the formal solution produces a ''rigid body'' reference frame (like a geodesic dome) with an *a priori* unknown overall rotation (consisting of a rotational offset at some epoch, and a time variable rotation) with respect to any ''standard'' coordinate system. One of the problems confronting the *Hipparcos* Project from the outset was how to determine the relationship between the *Hipparcos* Instrumental Reference Frame and an inertial or nearly-inertial (nonrotating) reference frame. The link to a non-rotating reference frame is necessary so that any conclusions reached from studies of the kinematics and dynamics of stellar motions derived with respect to the frame are not invalidated by contamination with spurious systematic motions introduced by the motion (rotation) of the reference frame itself.

The obvious choice was a Very Long Baseline Radio Interferometry (VLBI) reference frame, for several reasons. First, it is the most accurate available over the whole sky.

[1]McDonald Observatory, University of Texas at Austin, Austin, Texas 78712.
[2]Center for Space Research, Aerospace Engineering Department, University of Texas at Austin, Austin, Texas 78712.
[3]Department of Physics, University of Rhode Island, Kingston, Rhode Island 02881.
[4]Electronic mail: paul@skye.phys.uri.edu.
[5]Current address: United Space Alliance, Houston, TX.
[6]Cambridge University, Cambridge, England.
[7]Lowell Observatory, Flagstaff, Arizona.
[8]Space Telescope Science Institute, Baltimore, Maryland.
[9]University of Western Sydney, Nepean, Australia.
[10]Observatoire de Paris-Meudon, Meudon, France.
[11]Department of Astronomy, University of Virginia, Charlottesville, Virginia.
[12]Department of Astronomy, University of Texas at Austin, Austin, Texas 78712.
[13]U. S. Naval Observatory, Washington, D. C.
[14]Observatoire de las Cote d Azure/C.E.R.G.A., Grasse, France.
[15]Carnegie Observatories, Pasadena, California.
[16]Deceased.
[17]ESA, Noordwijk, The Netherlands.
[18]Jet Propulsion Laboratory, Pasadena, California.
[19]Department of Astronomy, Yale University, New Haven, Connecticut.

Second, it is indirectly accessible through optical counterparts of radio emitting objects, via several techniques. Third, the accurate "registration" of radio and optical images is critical for astrophysical understanding of many types of objects. The ultimate choice was mandated by the International Astronomical Union (IAU). In 1991, the IAU adopted a resolution specifying the conditions for the reference frame to be adopted by the astronomical community (Bergeron 1992). The result of this resolution was the definition of the International Celestial Reference System (ICRS); the ICRS comprises the axes of the reference frame which are fixed with respect to the system of extragalactic objects. The catalogue which gives the coordinates of 606 sources on the ICRS is the International Celestial Reference Frame (ICRF). The ICRF, as mandated by the IAU, was established and is maintained by the International Earth Rotation Service (IERS).

Several techniques have been used to obtain estimates of the rotation parameters. Lindegren & Kovalevsky (1995) have given an overview of the *Hipparcos* extragalactic reference frame link program, including the "uniform formalism" used to combine the results from each of the individual programs. The combination of the results of the different techniques to derive the final link is given in Kovalevsky *et al.* (1997). In this paper we give the details of the program to determine the link using the *Hubble Space Telescope* Fine Guidance Sensors.

2. THE *HST-HIPPARCOS* EXTRAGALACTIC LINK PROJECT: PREPARATIONS

In 1978, we realized that the Fine Guidance Sensors (FGS) of the *Hubble Space Telescope* (*HST*) could be used to measure the angular separations of stars from extragalactic objects (EGOs): Quasars, BL Lac Objects, and some active galactic nuclei (AGNs). The expected rms accuracy of a single separation was on the order of 2 or 3 mas. Discussions among the Astrometry Science Team (AST) of *HST*, the Input Catalogue Consortium (INCA) of the *Hipparcos* Project, the Project Scientist of *Hipparcos*, and the head of the Fundamental Astronomy by Space Techniques (FAST) data reduction consortium resulted in the proposal to use *HST* to make observations to be used to link *Hipparcos* to EGOs. NASA has continued to support this project in various ways, which are acknowledged at the end of the paper.

The choice of a reference frame for the *Hipparcos* link was (and still is) the VLBI frame, because it is the most accurate nearly-inertial frame available, and it provides benchmark objects with optical counterparts, whose positions are known at the milliarcsecond level. Because neither *Hubble* nor *Hipparcos* was yet built, we did not know the on-orbit operating characteristics or constraints. Therefore, we searched the available literature, including Very Large Array calibrator lists and VLBI structure lists, for suitable EGOs to use for the link. A list of about 170 objects was compiled.

The initial choice of candidate objects, both EGOs and *Hipparcos* stars, depended on many factors (Hemenway & Duncombe 1986). The Smithsonian Astrophysical Observatory (SAO) Star Catalogue (Smithsonian Institution, Washington, D.C., 1966) was searched for stars within 18.6 arcmin of the EGOs, and 414 candidate stars were chosen based on their brightness and nonduplicity, or unknown duplicity status. The list was submitted to the *Hipparcos* Project in 1982 as part of a program to determine the frame rotation. The project was accepted, and the list was accepted as provisional, to be reduced and adjusted as the operational capabilities of both satellites became better defined. In particular, duplicity of stars at the 0.1 to 10 arcsecond level affects the final *Hipparcos* accuracy, while duplicity at the 0.010 to 0.100 arcsec level affects the FGS's capability to determine a unique and accurate position, or to lock up on the star at all, depending on the separation, magnitude, and magnitude difference between the primary and secondary stars. Therefore an intensive program of groundbased speckle interferometry was undertaken to determine those candidate stars which showed no evidence of duplicity that was likely to affect the position derived from the FGS observations or the *Hipparcos* observations. Because the *Hipparcos* accuracy was expected to start to degrade at something fainter than 10th magnitude, only stars brighter than 11th were considered. The results of the southern speckle program are given by Argue *et al.* (1984, 1985). The results of the northern speckle program are given in the Appendix. Many of the stars were found to be double on the several hundredths of an arcsecond level and were rejected.

3. *HIPPARCOS*

3.1 Instrumentation

By 1984, the observing characteristics of the *Hipparcos* Satellite were becoming established. In particular, the total observing time available during a single pass of a field through the detector was known. The distribution of observing time available to stars of different magnitude within one field was determined. Bright stars required less time than faint stars. If a very faint star were given highest priority, then very bright stars in the same field might be rejected. The competing stars came from the various programs proposed for the *Hipparcos* Project in 1982. Some fields were affected by "veiling glare" from nearby bright stars, which contaminated the field and reduced the accuracy for stars in those fields. We began the long process of working with the *Hipparcos* Project to identify which of our stars could be observed accurately by *Hipparcos* and would be included in the "super high-priority" list for the reference frame link to extragalactic objects. Since the determination of the system rotation is vital to the final external accuracy and usefulness of the *Hipparcos* Catalogue, and because a relatively small number (of the order of 200 stars) is involved, the stars for this and other link projects (such as the radio stars to be observed directly with VLBI) were put in the special "super high-priority" category. Each of the *Hipparcos* fields including an EGO was carefully and individually analyzed for obtaining an *Hipparcos* observation of the link stars under the best possible conditions.

The *Hipparcos* Satellite was launched on 1989 August 8. The satellite was operated until 1993 August 15. The data reduction was performed by the two data reduction consor-

TABLE 1. *Hipparcos* star data.

Hipparcos Designation	INCA #	Right Ascension degrees	Declination degrees	V magnitude
INCA221-002	5588	17.91750	22.72214	7.53
INCA221-003	5673	18.22369	22.83844	8.28
INCA221-015	9131	29.42525	74.62493	9.36
INCA221-020	12845	41.28567	62.59201	9.50
INCA221-022	14978	48.26776	-77.02868	9.00
INCA221-027	19278	61.97152	-12.16017	11.44
INCA221-028	19290	62.02578	-12.15177	9.80
INCA221-008	21152	68.01977	5.41002	6.36
INCA221-029	21272	68.46022	5.38569	7.92
NEWHIP-053	25186	80.81462	-36.37191	8.40
INCA221-036	26586	84.76880	-44.11064	10.67
INCA221-039	31390	98.70996	-75.21888	9.00
INCA221-040	35542	110.01543	71.34637	9.50
INCA221-041	35654	110.35137	71.14843	9.60
INCA221-044	40935	125.30356	-12.82679	10.37
INCA221-050	42701	133.50224	20.23040	8.60
INCA221-053	45432	138.88820	29.79253	10.05
INCA221-057	48952	149.79580	32.43894	9.40
INCA221-061	53990	165.66561	-32.73820	10.67
NEWHIP-045	54136	166.13033	38.24136	6.02
NEWHIP-047	54210	166.38395	38.27585	8.72
INCA221-072	57935	178.22576	49.39594	9.70
INCA221-073	57984	178.40551	49.60048	11.24
INCA221-088	63896	196.42388	-10.50186	9.27
NEWHIP-057	66417	204.24625	24.61330	5.72
NEWHIP-033	67872	208.52396	63.87488	10.30
INCA221-092	68928	211.66810	28.48402	10.71
INCA221-093	68955	211.73282	28.43804	6.90
INCA221-097	70068	215.07659	54.50540	9.27
NEWHIP-034	70715	216.93885	23.84066	10.93
INCA221-098	71416	219.07416	63.46554	7.90
NEWHIP-035	71839	220.43495	35.24043	8.40
INCA221-104	74830	229.39556	-24.47722	9.90
NEWHIP-050	74850	229.43804	-24.42868	9.00
INCA221-105	74920	229.64951	-24.24920	8.50
NEWHIP-036	78029	238.98767	10.98717	10.80
INCA221-167	81888	250.90919	39.91766	9.77
NEWHIP-052	82589	253.24745	39.60562	9.81
INCA221-131	99260	302.24105	-49.07830	9.00
INCA221-139	106347	323.07744	-12.07153	10.53
INCA221-143	108795	330.60589	42.42543	8.44
INCA221-173	108857	330.78862	31.86585	9.32
INCA221-153	113060	343.44549	16.29195	10.28
INCA221-154	113115	343.59858	15.99728	9.65

INCA = Input Catalogue Original List Designation
NEWHIP = Hipparcos Stars added after HST launch. (See Text.)

tia: FAST and NDAC (the Northern Data Analysis Consortium).

3.2 The Hipparcos Data

The *Hipparcos* data that we used for the frame rotation are the data for our *Hipparcos* stars from the ''final'' combined NDAC and FAST consortia solutions to the raw *Hipparcos* data. The solution is known as the ''H37'' solution, meaning that it is the *Hipparcos* (H) solution from the full 37 months of data used in the final solution. The H37 solution was made with respect to the FK5, as described by Lindegren & Kovalevsky (1995), but may not represent the ''true'' FK5 because of the selection of FK5 stars used in the solution. (Certain double stars and other stars were omitted.) Also, the FK5 is known to have complex, probably magnitude and color-dependent, zonal errors so that the *Hipparcos* Catalogue can only coincide with the FK5 in some general manner. The various groups working to form the frame link were given the H37 data relevant to their stars. Each group determined the rotation to the ICRF, using its own technique.

Table 1 gives the *Hipparcos* stars in our sample. The positions are not the final *Hipparcos* catalogue positions and should be used for identification purposes only.

4. THE *HUBBLE SPACE TELESCOPE* FINE GUIDANCE SENSORS

4.1 Instrumentation

The FGSs are optical interferometers that use light from the focal surface of *HST* to derive positions within the focal surface structure (Benedict *et al.* 1992). Three areas on the sky, henceforth referred to as ''pickles'' (Fig. 1), are accessible to three FGS instruments, located in radial bays on *HST*. The FGS in bay 3 (FGS3) is the one designated as the astrometer (Benedict *et al.* 1992), and has been calibrated for astrometry. The area available in the pickle is about 67 square arcminutes. The maximum measurable separation between two objects is about 18.6 arcmin along the ''long axis'' of the pickle. The FGS interferometer is a nulling device, with a 5 arcsec square aperture, and a transfer function (Fig. 2) with a useful width of about 40 milliarcseconds for a single object. Two perpendicular transfer functions provide settings in x and y internal FGS coordinates, precise to better than one mas. (Note that the single setting measuring *accuracy* is significantly worse than this precision.) Only one target can be observed at a time with the astrometer, so several settings are made during an orbit on several targets within a field. These usually include the primary target or targets, a set of background reference stars, and, when necessary, a set of repeat measurements on some check stars throughout the observing session, to measure drift. The operation of the FGS for astrometry has been described in several places (cf. Benedict *et al.*1994, and references therein). A description of some peculiarities which appear in our data will illustrate the problems we faced in reducing and understanding our data.

To acquire an object in the FGS, the aperture is moved in a 5 arcsec diameter circle around the expected position of the target. After this ''nutation circle'' is completed, the ''total power'' variation is used to improve the estimated location for the target in the FGS frame, and the FGS aperture is moved along the new circle. The process is repeated for a certain length of time (a certain number of circles). At the end of this ''coarse track,'' a position is estimated that is good to about 0.1 arcsec. The FGS aperture is then ''backed off'' from this expected position, and slowly stepped on a diagonal track (the ''walkdown''), and the Fine Error Signal (FES) is measured at each step in each coordinate. The FES is the interferometer response for targets somewhere within the interference transfer function. Figure 3 shows a plot of a typical motion of the FGS aperture in the FGS coordinate system. Figure 4 shows the walkdown in more detail plus the fine lock. Figure 5 shows the ''jitter ball'' of fine lock in more detail.

When three successive values above a preset threshold are recorded on one axis, the FGS is assumed to have ''found'' the transfer function on that axis, and the FGS goes into ''fine lock'' on that axis. The process is continued on the other axis until ''fine lock'' is achieved on the second axis also. (If the transfer function is ''missed'' because the target is too faint, or too extended, or because of large jitter in the system, the observation will be aborted when the ''walkdown'' exceeds a preset number of steps in either axis.) Fine Lock consists of measuring the FES during one sample time,

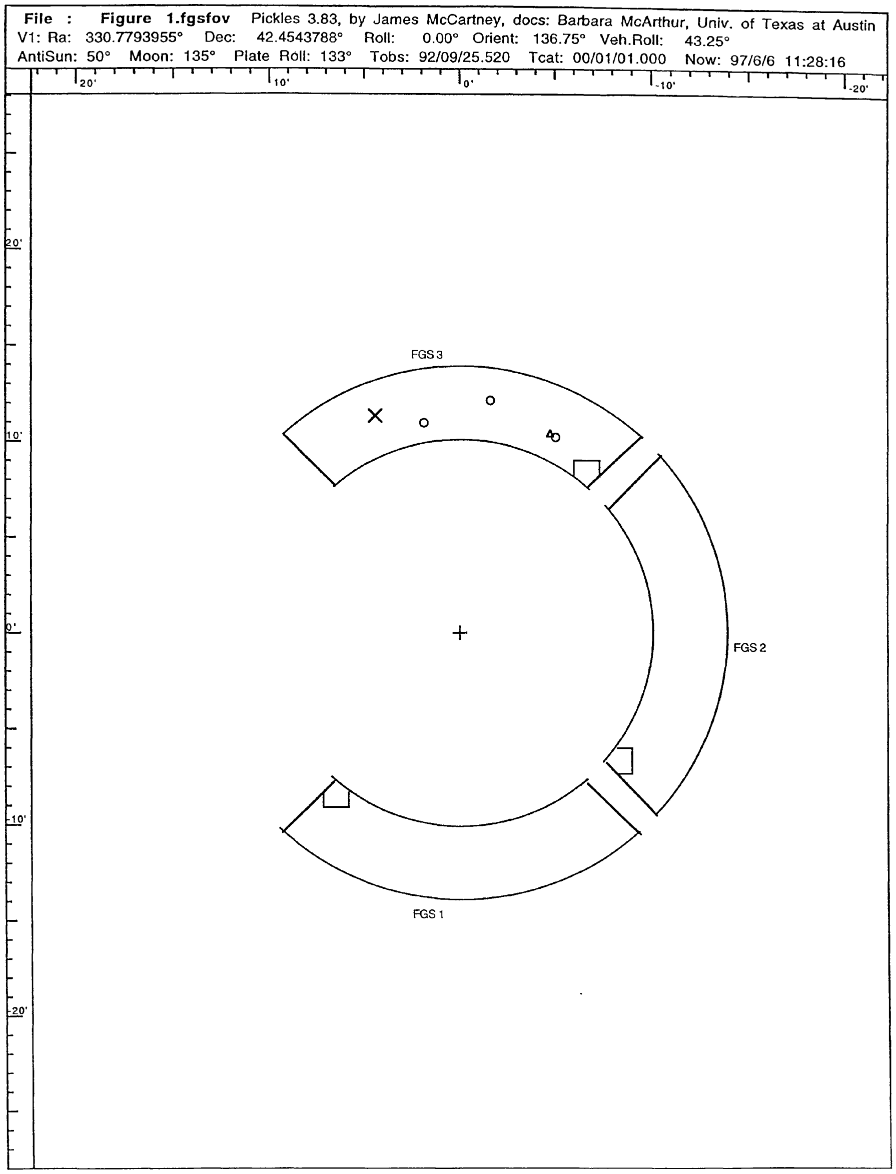

FIG. 1. Schematic view of the *HST* "focal plane" with the positions of the three Fine Guidance Sensor Fields of View. The inner radius is approximately 10 arcminutes and the outer radius is approximately 14 arcmin. The "*x*" marks INCA221-172 and the triangle marks 2200+420. The circles mark 3 "reference stars" at about 14th magnitude.

determining where on the transfer function the target is located, and deriving a correction to be applied to the FGS to bring the target back to the null of the transfer function. The sample time is fixed for each target, and may be a power of 2 multiple of the basic sample rate of 40 Hz. The raw data consist of the star selector encoder readings of the positions of the 5 arcsec aperture with respect to the FGS reference frame, which is then related to the *HST* reference frame and ultimately to the sky through the two guiding FGSs. Averaging the *xy* positions in the FGS frame produces a single position for each target for each setting of the FGS. A typical FGS "position" will be derived from upwards of 6000 individual data points. Plots of the *xy* distribution (jitter balls) and time variation of these data often indicate why a particular data set will have high residuals, either in the "drift solutions" or the final system solutions. (See the discussion below.) Figure 6 shows a "dumbbell" shape, characteristic of jitter balls after a day-night *HST* transition. This shape often occurred after the replacement of the solar panels but before the installation of the software (SAGA II) to reduce the jitter associated with the new solar panels.

Originally, the expected nominal operating range of the FGSs was between 9th and 17th V magnitude, with an extension to 4th magnitude with a neutral density filter in an almost-collimated beam within the FGS. We investigated the detailed photometric history of as many as possible of our candidate EGOs to try to get the optimum selection (Bozyan *et al.* 1990). After the launch of *HST* in 1990, and with the

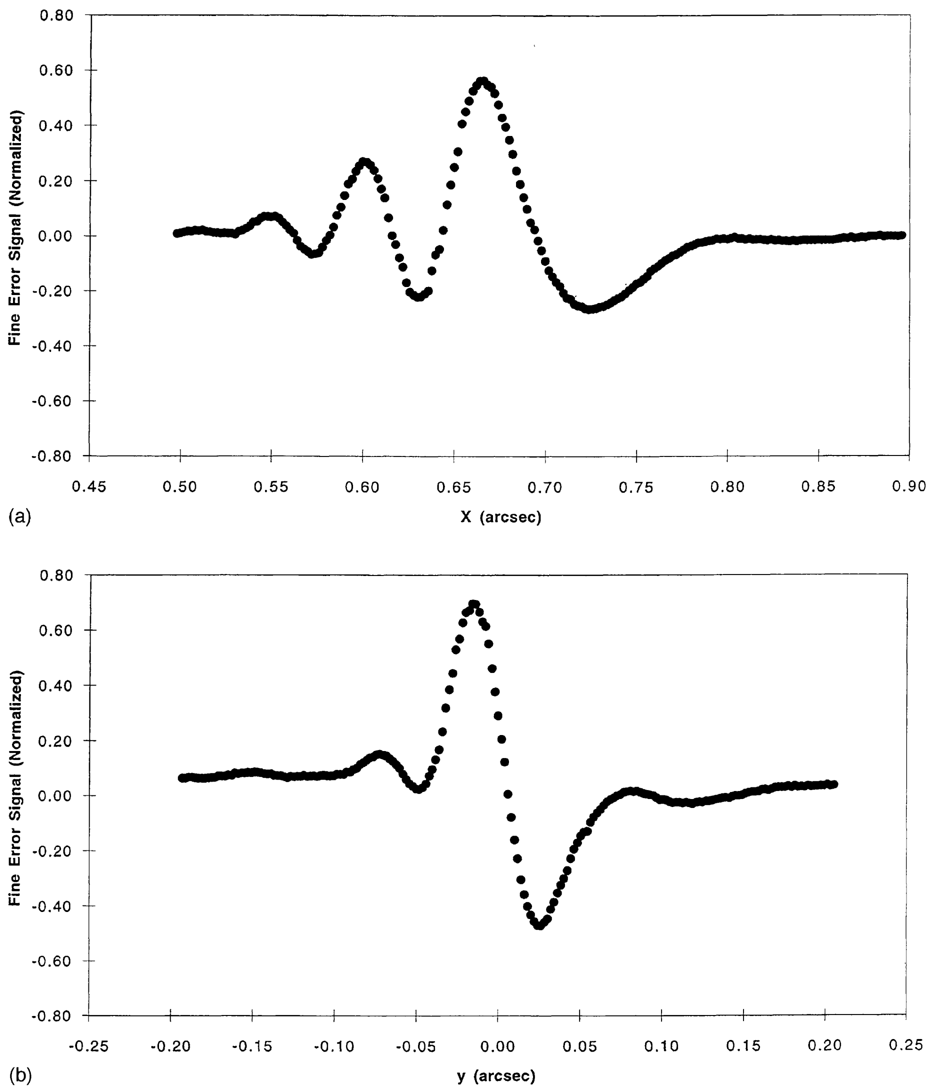

FIG. 2. The response of the FGS interferometer as a function of angular offset of the target from the "null" position. The overall response is known as the "transfer function" of the FGS. (a) x axis. (b) y axis. The data were taken on star Upgren 69 in NGC 188, which is the standard transfer function calibration target. The data have been binned and averaged over several scans.

identification of the spherical aberration due to the misfiguring of the primary mirror, the limiting magnitude of the FGS was determined to be closer to 15.5 mag than 17, as originally envisaged. Because of the steep increase in numbers of EGOs with magnitude, many of our best VLBI EGOs could not be observed with the FGS. Therefore, a fast and massive search was initiated to find any optical EGOs which were small enough and bright enough to be observed (locked onto with the FGS interferometer) by *HST*. Most of the EGOs were catalogued sources in the northern hemisphere, but an intensive radio and optical program in the south turned up several new likely QSOs and AGNs, which were included in the initial observing list for *HST* (cf. White & Jauncey 1988, for example). Adding new stars into the *Hipparcos* Input Catalogue was impossible at that late stage, so we were limited to searching around the new EGOs for stars in the existing *Hipparcos* Input catalogue. About 60 pairs were identified, of which about 20 have been observed.

4.2 Calibration

The calibration of FGS3 for astrometry, including the Optical Field Angle Distortions (OFAD), is described in Whipple *et al.* 1996. As observations accumulated, new solutions for the OFAD, and particularly a time-variable OFAD, were obtained. We would rerun all of our data sets with the revised calibrations. The results usually provided improved solutions, but they also provided the *HST* Astrometry Science Team with a "sanity check" on the new solutions.

While most FGS observations are made using the clear (F583W) filter, observations of the brighter *Hipparcos* stars were made with the neutral density (F5ND) filter. In order to determine the positional offset of the neutral density filter with respect to the clear filter, a special set of observations was performed.

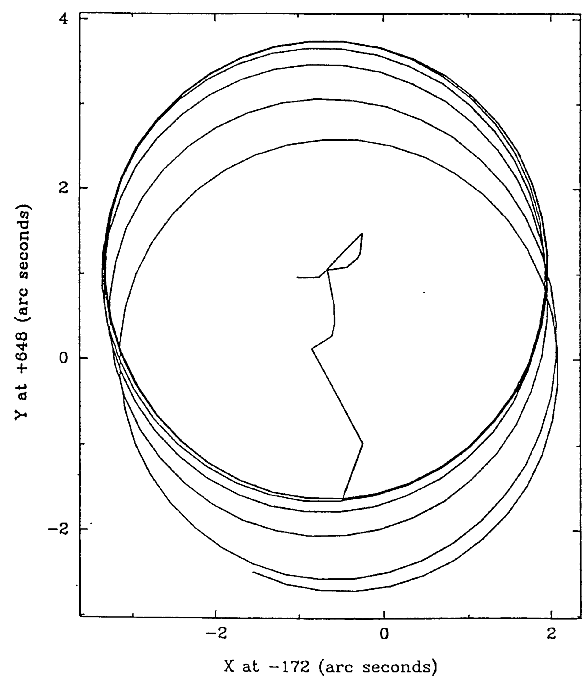

FIG. 3. Path of the FGS square aperture during an entire observation of one object.

4.3 Data

For this project, where we measured the separation of two targets (an *Hipparcos* Star and an EGO) in one pickle, we devised an observing routine that allows us to keep track of small continuous changes (drift) in the FGS coordinate system (due to thermal effects during a 20 min observing session, for example), and obtain several observations of both targets of interest. The basic observing sequence is

EGO-Ref1-Ref2-Ref3-
Hip*-EGO-Hip*-
Ref3-Ref2-Ref1-EGO,

where EGO is the extragalactic object, Hip* is the *Hipparcos* star, and, Ref*n* is the *n*th reference star in the field. Note

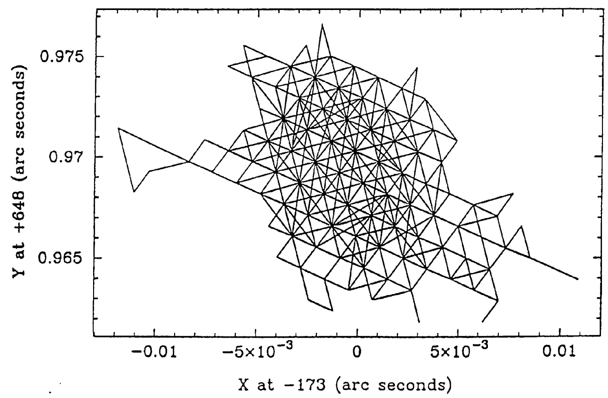

FIG. 5. Motion of the FGS aperture while the target was in fine lock in both x and y. The final measured position was derived from the mean position in x and y after fine lock in both axes was achieved.

that here "reference star" simply refers to a field star which serves as a local reference in the xy frame, and whose position is not expected to be known to better than a few arcseconds.

In our observing sequence, every target that is successfully observed more than once is used in the determination of the FGS reference frame drift.

4.3.1 Data from the FGSs themselves: Background and the FES

One problem we encountered was the way in which the FGS computes the FES. After initial acquisition of a target, the FGS steps the aperture across the field, searching for the interferometer transfer function of the target ("looking for fringes"). The FGS electronics uses data from the start of this "walkdown" to determine a background level which is used in the calculation of the FES when the target is within the inner portion of the transfer function. For faint targets (say 14.5 mag and fainter), the determination of the background is dominated by photon statistics. We have devised and implemented a procedure where extensive data from the walkdown are used to derive a more accurate background.

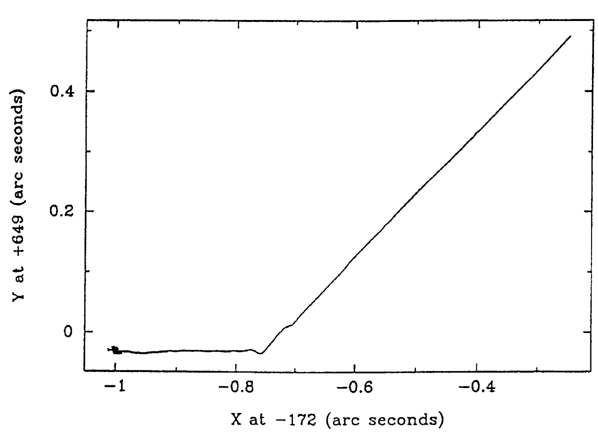

FIG. 4. Path of the FGS aperture during walkdown and acquisition of the target in fine lock, first in y and then in x.

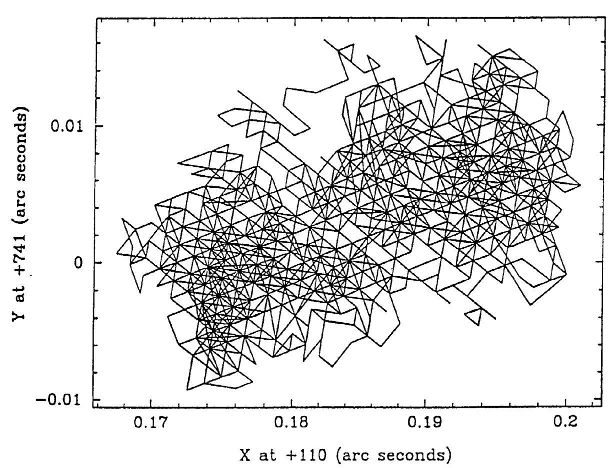

FIG. 6. A "dumbbell" jitterball from a disturbed *HST* platform.

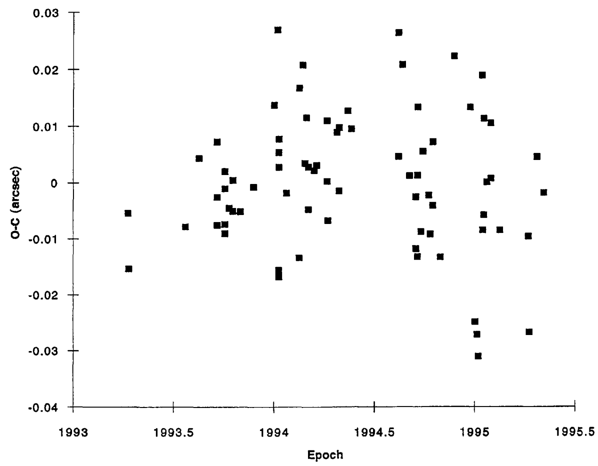

FIG. 7. O-C residuals vs time for an early solution without a time-variable plate scale.

The level of the interferometer null is determined more accurately using this background. We reprocessed all the FGS data using the new null, and, for fainter sources, found shifts of several milliarcseconds in many cases.

4.3.2 *Data from a moving FGS within HST: Drift during an observation set*

Often, the FGS astrometer coordinate system moves relative to the guiding coordinate system during an observation set, on the order of 10 milliarcseconds or more over periods up to 40 min (cf. Benedict *et al.* 1994). The cause of the motion is not known, but is suspected to be due to thermal, and/or mechanical shifts within the FGSs and within the *HST* support structures. We have found two drift models which seem to work well for our data under different circumstances. The first is a quadratic drift in time, where the functional form is

$$x(t)=x(t_0)+a(t-t_0)+b(t-t_0)^2$$

and similarly for y; i.e., we solve for a simple quadratic variation in each coordinate with time.

The second model is a "rotation" model where we assume that the FGS coordinate system is moving with a linear drift superimposed on a constant rotation, so that we solve for drift rates in x and y, and an angular velocity term for the frame rotation rate.

We used the following method to select between the two drift models. For a given observation set, the data are fitted to each drift model independently. The target positions are determined in the FGS reference frame at the beginning of the observation set for each drift model. Two EGO-*Hipparcos* star separations are determined from these positions. The difference between the solved-for separations is calculated. The standard deviations of the 5 targets in x and y are added in quadrature to get a "goodness of fit" for each solution. The model with the best (lowest) "goodness of fit" is then used to correct for the drift.

4.3.3 *Data from a changing HST: Time variable OFAD*

In 1993 December, a set of observations was made at 20 closely spaced *HST* pointings, measuring about 60 individual stars in order to calibrate the Optical Field Angle Distortions (OFAD) in the Astrometer FGS. The field is in the open cluster M35. A full overlapping plate solution provides the means to determine the OFAD to an accuracy commensurate with the measuring accuracy of the FGS, but depending on the form of the OFAD model within the pickle and the de-

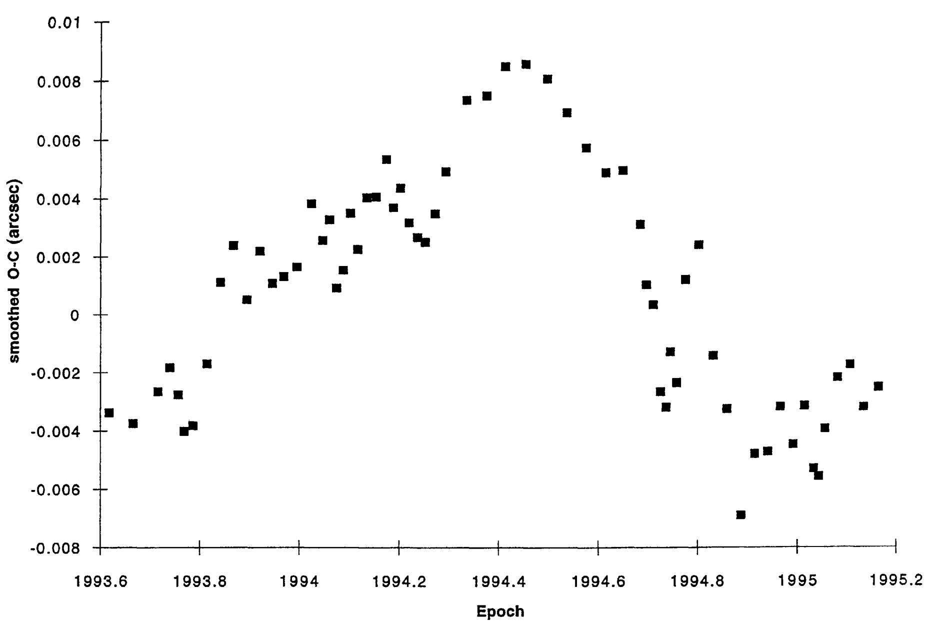

FIG. 8. 10 point running boxcar smoothing of Fig. 7.

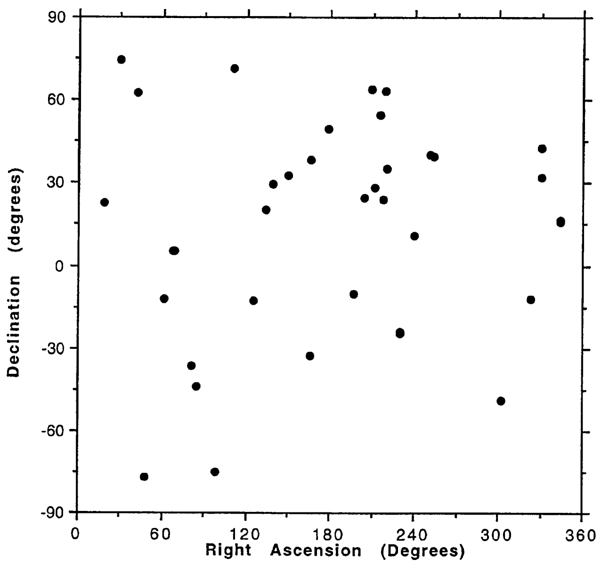

FIG. 9. Distribution on the sky of the pairs used in the final link solution.

tailed distribution of the stars observed. We monitor changes in the OFAD by measuring one subfield periodically. Soon we discovered that the field distortions were changing at a rate of up to a milliarcsecond per month in some parts of the field. Analysis has provided us with some possible physical causes of these changes, but the changes are not yet fully understood. However, mathematically, we have derived a time-variable OFAD (TVO) which calibrates most of the changing distortions. Whenever we determine a new TVO, it is applied to all the data. When the first TVO was applied to our data in 1994 December, our mean residual from the *Hipparcos* link rotation fit went from 30 mas for a static OFAD to 10 mas for the first TVO.

4.3.4 Data from a changing HST: Time variable scale in our data

Figure 7 shows a plot of the O-Cs vs time from an early solution for the link frame rotation. The parameters in the model contained only the link rotation parameters (see below) and an FGS scale. A nonlinear change is apparent in the data. Figure 8 shows a 10 point running boxcar average of the data.

We tried to fit both a quadratic and a sinusoidal variation to the data with about equal success. We chose to implement a scale change that is quadratic in the time. The parameters show up as "scalefact," "scaledot," and "scaleddot." The units are: unitless, 1/time, and 1/time-squared.

5. THE *HST HIPPARCOS* VLBI LINK PROJECT

5.1 Theory

The basic problem is to measure the rotational offset of the *Hipparcos* reference frame with respect to a defined VLBI frame at a particular epoch, and to measure the time variation of that rotational offset. The basic FGS datum is a measurement of the separation between a *Hipparcos* star and an EGO at the epoch of observation. We use a formulation that computes the difference between the sine of the separation observed with *HST* and the sine of the separation as computed using the VLBI catalogue position for the EGO and the *Hipparcos* star position at the epoch of the *HST* observation. The position, proper motion, and parallax of the *Hipparcos* star come from the H37 "preliminary" catalogue supplied to us by the *Hipparcos* Project. The equation of condition is

$$\mathrm{O-C} = \sin(S_{\mathrm{FGS}}\rho_{\mathrm{FGS}}) - |\mathbf{X}_{\mathrm{VLBI}} \times \mathbf{R}\mathbf{X}_{\mathrm{HIP}}|_{\mathrm{CAT}}, \tag{1}$$

where: O−C=Observed minus Computed difference of sines, $S(t)_{\mathrm{FGS}}$=FGS Scale factor at the *HST* epoch of observation, ρ_{FGS}=Observed angular separation with *HST*, $\mathbf{X}_{\mathrm{VLBI}}$=VLBI position unit vector, $\mathbf{R}(t)$=Rotation matrix at *HST* epoch, *from* HIP *to* ICRS, $\mathbf{X}_{\mathrm{HIP}}$=Hipparcos Catalogue Position unit vector at the *HST* epoch of observation, and CAT refers to data derived from catalogue information.

The Rotation Matrix, $\mathbf{R}(t)$ is made up of two parts, a rotational offset at some epoch t_0: $\mathbf{R}(t_0)$ and a time variable rotation rate $\dot{\mathbf{R}}$ times the epoch difference $(t-t_0)$:

$$\mathbf{R}(t) = \mathbf{R}(t_0) + (t-t_0)\dot{\mathbf{R}}. \tag{2}$$

We used the following formulation:

$$\mathbf{R}(t_0) = \begin{pmatrix} 1 & \alpha & \beta \\ -\alpha & 1 & \gamma \\ -\beta & -\gamma & 1 \end{pmatrix} \tag{3}$$

and similarly for $\dot{\mathbf{R}}$.

The *Hipparcos* Project used a formulation where our (α,β,γ) are replaced by $(\varepsilon_3, -\varepsilon_2, \varepsilon_1)$ and similarly $(\dot{\alpha},\dot{\beta},\dot{\gamma})$ with $(\omega_3, -\omega_2, \omega_1)$. The epsilons are small (of the order of

TABLE 2. Extragalactic object data.

EGO Name	Right Ascension degrees	Declination degrees	Right Ascension variance radians^2	Declination variance radians^2	Source
0109+224	18.0242697	22.7441073	1.08E-14	1.85E-14	VLBI
0153+744	29.3956871	74.7120083	1.00E-14	7.42E-15	VLBI
0241+622	41.2404035	62.4684764	6.70E-13	2.64E-13	VLBI
0312-770	47.9802097	-76.864125	4.38E-14	3.46E-14	VLBI
0405-123	61.9517957	-12.193517	5.20E-13	1.17E-13	VLBI
0430+052	68.2962315	5.35433878	2.36E-13	5.26E-13	VLBI
0521-365	80.7416027	-36.45857	1.46E-14	8.67E-14	VLBI
0537-441	84.7098398	-44.085816	1.42E-13	3.60E-13	VLBI
0637-752	98.9437831	-75.271338	5.66E-15	5.63E-15	VLBI
0716+714	110.472702	71.3434343	5.98E-15	6.05E-15	VLBI
0818-128	125.239365	-12.983103	1.39E-14	1.63E-14	VLBI
0851+202	133.703646	20.1085114	4.96E-15	5.22E-15	VLBI
0912+297	138.96834	29.5566785	1.35E-14	2.51E-14	VLBI
0955+326	149.58729	32.4006137	1.19E-14	1.70E-14	VLBI
1101+384	166.113808	38.2088331	1.63E-14	2.09E-14	VLBI
1101-325	165.88136	-32.854637	5.02E-14	2.58E-13	VLBI
1150+497	178.351944	49.5191195	9.48E-15	1.06E-14	VLBI
1302-102	196.387563	-10.555397	6.71E-15	8.40E-15	VLBI
1334+246	204.328032	24.384242	7.72E-08	7.72E-08	optical
1351+640	208.315745	63.762448	7.72E-08	7.72E-08	optical
1404+286	211.751643	28.4540805	3.49E-14	9.51E-14	VLBI
1418+546	214.944156	54.3874409	5.66E-15	5.63E-15	VLBI
1424+240	216.751633	23.8000097	7.75E-14	1.71E-13	VLBI
1435+638	219.190842	63.6105185	7.90E-15	8.40E-15	VLBI
1440+356	220.531098	35.4397006	3.09E-09	3.09E-09	optical
1514-241	229.424221	-24.372077	9.74E-15	9.45E-15	VLBI
1553+113	238.93007	11.18927	7.72E-06	7.72E-06	optical
1641+399	250.745041	39.8102761	8.48E-14	8.35E-14	VLBI
1652+398	253.46757	39.7601691	5.43E-15	6.49E-15	VLBI
2005-489	302.355795	-48.831589	3.11E-12	4.19E-12	optical
2128-123	322.896924	-12.117999	7.67E-14	2.18E-13	VLBI
2200+420	330.680381	42.2777722	4.14E-14	5.84E-14	VLBI
2201+315	330.812399	31.7606306	1.45E-14	2.17E-14	VLBI
2251+158	343.490616	16.1482114	1.00E-13	1.45E-13	VLBI

TABLE 3. *HST* separation data.

Ego Name (IAU-1950)	Hip Name	HST Epoch	Measured HST Scaled Sep.(O) (")	HST est. meas. err. (mas)	RotCATSep (C) (")	O-C (mas)	O-C expected (expect. err) (mas)	Individual Chi2
0109+224	INCA221-2	1993.90042	363.2958	1.54	363.3031	-7.30	4.84	2.28
0109+224	INCA221-2	1994.89747	363.3315	2.04	363.3273	4.19	6.57	0.41
0109+224	INCA221-3	1993.56078	743.8005	3.34	743.8094	-8.90	5.19	2.94
0153+744	INCA221-15	1994.77900	314.7257	1.09	314.7221	3.57	9.18	0.15
0241+622	INCA221-20	1993.79866	451.0179	1.93	451.0269	-8.97	10.65	0.71
0241+622	INCA221-20	1994.79277	451.0221	5.33	451.0210	1.10	15.19	0.01
0312-770	INCA221-22	1994.74473	636.6662	1.14	636.6780	-11.78	5.69	4.29
0405-123	INCA221-27	1994.02565	138.6907	2.24	138.6986	-7.91	18.90	0.17
0405-123	INCA221-27	1994.02602	138.6916	1.82	138.6986	-7.05	18.86	0.14
0405-123	INCA221-27	1994.12723	138.6917	3.88	138.6998	-8.10	19.81	0.17
0405-123	INCA221-27	1995.04826	138.7056	2.25	138.7101	-4.55	25.59	0.03
0405-123	INCA221-28	1994.02565	300.5850	1.86	300.5806	4.44	17.48	0.06
0405-123	INCA221-28	1994.02602	300.5870	1.63	300.5806	6.42	17.45	0.14
0405-123	INCA221-28	1994.12723	300.5909	3.46	300.5794	11.48	18.38	0.39
0405-123	INCA221-28	1995.04826	300.5847	1.88	300.5736	11.15	23.62	0.22
0430+052	INCA221-29	1994.97940	597.9445	1.56	597.9256	18.96	21.99	0.74
0430+052	INCA221-8	1993.75870	1010.6796	2.40	1010.6924	-12.79	6.41	3.98
0430+052	INCA221-8	1994.67547	1010.6000	3.29	1010.5907	9.35	8.55	1.20
0521-365	NEWHIP-53	1994.02622	376.9667	2.75	376.9631	3.59	5.84	0.38
0537-441	INCA221-36	1993.72019	176.6693	2.49	176.6780	-8.70	6.64	1.72
0537-441	INCA221-36	1993.75759	176.6735	2.14	176.6782	-4.61	6.59	0.49
0537-441	INCA221-36	1993.83481	176.6756	24.93	176.6780	-2.39	25.73	0.01
0537-441	INCA221-36	1994.70649	176.6753	2.18	176.6766	-1.27	8.64	0.02
0537-441	INCA221-36	1994.71532	176.6734	3.46	176.6766	-3.23	9.07	0.13
0537-441	INCA221-36	1994.83119	176.6759	2.72	176.6767	-0.72	9.03	0.01
0537-441	INCA221-36	1995.73338	176.6723	3.00	176.6753	-3.00	11.12	0.07
0637-752	INCA221-39	1993.27764	285.7385	2.83	285.7402	-1.70	3.87	0.19
0637-752	INCA221-39	1994.32451	285.7488	2.40	285.7529	-4.10	4.58	0.80
0637-752	INCA221-39	1995.31245	285.7592	2.15	285.7644	-5.13	5.54	0.86
0716+714	INCA221-40	1993.79832	526.6672	1.73	526.6673	-0.12	3.06	0.00
0716+714	INCA221-40	1994.79160	526.6709	2.41	526.6636	7.33	3.90	3.54
0716+714	INCA221-40	1995.79068	526.6610	3.04	526.6599	1.14	4.75	0.06
0716+714	INCA221-41	1994.00319	715.9023	1.35	715.8920	10.30	7.31	1.98
0716+714	INCA221-41	1995.00367	715.8999	2.17	715.8927	7.16	9.94	0.52
0818-128	INCA221-44	1995.12689	606.1793	2.31	606.1773	2.03	18.63	0.01
0851+202	INCA221-50	1994.21415	809.9516	3.62	809.9587	-7.10	9.16	0.60
0912+297	INCA221-53	1994.15482	885.2996	3.88	885.2979	1.73	6.81	0.06
0955+326	INCA221-57	1995.01873	648.4219	1.78	648.4414	-19.55	12.50	2.45
1101+384	NEWHIP-45	1994.06244	126.0189	2.81	126.0195	-0.56	4.22	0.02
1101+384	NEWHIP-45	1995.06171	125.9951	2.27	125.9958	-0.69	4.79	0.02
1101+384	NEWHIP-47	1995.01287	799.8591	1.38	799.8740	-14.91	6.16	5.86
1101-325	INCA221-61	1995.03859	775.9116	2.58	775.8856	25.96	14.62	3.15
1150+497	INCA221-72	1994.17231	532.7841	3.61	532.7903	-6.25	6.45	0.94
1150+497	INCA221-73	1994.16385	318.1586	2.19	318.1545	4.10	9.74	0.18
1150+497	INCA221-73	1994.20131	318.1534	3.06	318.1502	3.20	10.11	0.10
1302-102	INCA221-88	1994.27019	231.5948	1.15	231.5997	-4.95	8.16	0.37
1302-102	INCA221-88	1995.27456	231.5777	1.09	231.5845	-6.78	10.76	0.40
1334+246	NEWHIP-57	1993.35493	866.9880	4.07	867.0664	-78.35	4.69	0.00
1334+246	NEWHIP-57	1993.35493	866.9880	4.07	867.0664	-78.35	4.69	0.00
1334+246	NEWHIP-57	1994.34789	866.9918	3.05	867.0735	-81.70	4.54	0.26
1334+246	NEWHIP-57	1995.31404	866.9924	3.57	867.0800	-87.62	5.65	1.59
1351+640	NEWHIP-33	1994.20077	521.8641	2.10	522.7552	-891.02	6.21	0.00
1351+640	NEWHIP-33	1995.21620	521.8902	1.39	522.7746	-884.37	7.91	0.44
1404+286	INCA221-92	1995.08252	285.5403	3.97	285.5185	21.80	11.53	3.57
1404+286	INCA221-93	1995.04281	83.1640	2.18	83.1695	-5.56	5.08	1.20
1404+286	INCA221-93	1995.08252	83.1707	2.93	83.1708	-0.15	5.48	0.00
1418+546	INCA221-97	1994.26539	506.9555	3.25	506.9523	3.25	6.02	0.29
1418+546	INCA221-97	1995.26998	506.9072	3.26	506.8940	13.26	7.45	3.16
1424+240	NEWHIP-34	1994.14494	632.2960	2.32	632.2817	14.29	11.19	1.63
1424+240	NEWHIP-34	1994.17212	632.2661	1.43	632.2673	-1.24	11.10	0.01
1435+638	INCA221-98	1993.27369	554.4702	2.52	554.4655	4.73	3.63	1.70
1435+638	INCA221-98	1994.32569	554.4625	2.41	554.4541	8.40	4.54	3.42
1435+638	INCA221-98	1995.34537	554.4518	2.55	554.4431	8.72	5.68	2.36
1440+356	NEWHIP-35	1993.33860	771.1128	2.20	771.0663	46.47	3.66	0.00
1440+356	NEWHIP-35	1994.33449	771.1688	1.40	771.1244	44.45	4.43	0.00
1440+356	NEWHIP-35	1995.33791	771.2284	1.07	771.1829	45.49	5.61	0.02
1440+356	NEWHIP-35	1995.33791	771.2284	1.07	771.1829	45.49	5.61	0.02
1514-241	INCA221-104	1994.36940	390.0312	2.56	390.0508	-19.65	15.28	1.65
1514-241	INCA221-105	1994.38537	861.1732	1.32	861.1589	14.31	8.70	2.71
1514-241	NEWHIP-50	1994.36885	208.8680	5.61	208.8628	5.25	13.02	0.16
1553+113	NEWHIP-36	1994.37233	759.5412	2.21	755.9954	3545.84	21.32	0.00
1553+113	NEWHIP-36	1995.38182	759.6952	2.26	756.1556	3539.57	28.03	0.03
1641+399	INCA221-167	1994.26525	595.7653	29.66	595.7501	15.18	30.17	0.25
1652+398	NEWHIP-52	1994.31467	825.7527	0.62	825.7423	10.43	6.50	2.57
2005-489	INCA221-131	1994.64549	928.7516	1.83	928.7596	-8.01	7.28	0.00
2005-489	INCA221-131	1995.64186	928.7719	2.25	928.7820	-10.08	9.35	0.03
2128-123	INCA221-139	1993.75810	657.0638	1.32	657.0663	-2.47	17.47	0.02
2128-123	INCA221-139	1994.63997	657.0908	2.24	657.0643	26.57	23.44	1.28
2200+420	INCA221-143	1993.77994	567.2751	1.67	567.2859	-10.79	4.54	5.66
2200+420	INCA221-143	1994.77054	567.2852	1.88	567.2837	1.49	6.06	0.06
2200+420	INCA221-143	1995.67769	567.2713	2.47	567.2820	-10.68	7.63	1.96
2201+315	INCA221-173	1993.62936	385.7599	1.46	385.7617	-1.80	6.45	0.08
2201+315	INCA221-173	1994.62179	385.7875	2.21	385.7807	6.76	9.05	0.56
2251+158	INCA221-153	1994.74263	540.4336	1.32	540.4218	11.81	10.88	1.18
2251+158	INCA221-154	1994.73290	659.4009	0.65	659.3931	7.76	10.37	0.56

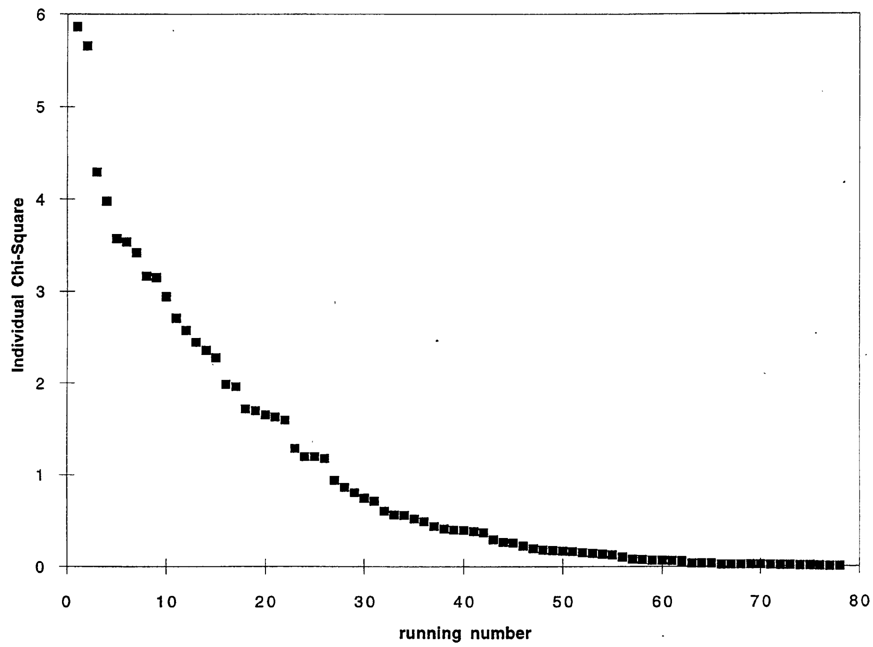

FIG. 10. Individual χ^2 values for the observed separation vs the number when sorted by size.

10 mas) rotations about the (x,y,z) axes while the omegas are the time derivatives of the epsilons.

For targets which have no VLBI position, but which give good separation measurements, we use differences of the (O−C)s between two epochs separated by a large fraction of a year or more. The change in separation with time is used to help solve for the matrix $\dot{\mathbf{R}}$, which describes the time-variable portion of the frame rotation, and is independent of the EGO position and the rotational offset matrix $\mathbf{R}(t_0)$ to second order. Seven separation differences involving 5 non-VLBI EGOs were included in the final solution.

Many types of observation go into the equation of condition. The measured *HST* separation, of course, but also the *Hipparcos* position, proper motion and parallax, and the VLBI positions are all observables in the sense that they were derived from observations and have associated errors and covariances. We use the least-squares system Gaussfit (Jefferys *et al.* 1988) to reduce our data. The input data for the equation of condition given are those data described above with their attendant uncertainties. Thus, the uncertainties in the VLBI and *Hipparcos* catalogues contribute directly to the final uncertainties that are computed.

The parameters of the model we solve for are the rotational offset (α,β,γ), the time variable rotation $(\dot{\alpha},\dot{\beta},\dot{\gamma})$, and the variable scale parameters (scalefact, scaledot, scaleddot).

5.2 Data

Here we present the data for the targets that were used in the final system solution which was sent to the *Hipparcos* Project. Figure 9 shows the distribution on the sky of the pairs used in the final solution. The data are presented in three tables. Table 1 contains the *Hipparcos* star information. Table 2 contains the EGO information. Table 3 contains the *HST* observed separation and fit solution information for the individual data points.

The columns for Table 1 (the *Hipparcos* Star data) are: (1) Designation, (2) the Input Catalogue number, (3) Right Ascension (Equinox=J2000) in degrees, (4) Declination (Equinox=J2000) in degrees; (5) V magnitude as given in the Input Catalogue.

The columns for Table 2 (the EGO data) are: (1) EGO Name in 1950 IAU notation; (2) EGO Right Ascension (J2000) in degrees; (3) EGO Declination (J2000) in degrees; (4) EGO R.A. variance in (radians)^2; (5) EGO Dec. variance in (radians)^2; (6) Source of positional data (VLBI=ICRS, optical=an optical catalogue and used for the time variable rotation only).

The columns for Table 3 (the observed *HST* separation data and solution residuals) are: (1) EGO Name; (2) *Hipparcos* Star Name; (3) *HST* observation epoch; (4) Post-solution scaled *HST* observed separation (O) in arcseconds; (5) Expected error in mas; (6) Separation computed (C) from the Rotated *Hipparcos* Catalogue positions at the epoch of *HST* observation, with parallax and proper motions applied, and the EGO positions given in Table 2; (7) the (O−C) residual from the final fit; (8) The "expected" error computed from the contributions of the individual error estimates of the constituents taken in quadrature (cf. Eichhorn 1974); (9) Individual χ^2 (see the text).

5.3 Analysis

System link solutions were made using artificial data to test the software as early as 1992 (Shattuck 1992). Improved software was used to make the first link solution with pre-

TABLE 4. Rotation parameters, formal errors, and covariances.

	Difference From the Final Combined Solution.								
	γ = ε_1 (mas)	β = $-\varepsilon_2$ (mas)	α = ε_3 (mas)	$\dot{\gamma}$ = ω_1 (mas/yr)	$\dot{\beta}$ = $-\omega_2$ (mas/yr)	$\dot{\alpha}$ = ω_3 (mas/yr)	scalefact (unitless)	scaledot (/yr)	scaleddot (/yr^2)
	-6.10	-3.25	+5.42	-1.60	-1.92	+2.26	0.99972271	1.3968E-05	0.00001757
	1994.25 solution:								
	σ_γ $=\sigma_{\varepsilon 1}$	σ_β $=\sigma_{\varepsilon 2}$	σ_α $=\sigma_{\varepsilon 3}$	$\sigma_{\dot{\gamma}}$ $=\sigma_{\omega 1}$	$\sigma_{\dot{\beta}}$ $=\sigma_{\omega 2}$	$\sigma_{\dot{\alpha}}$ $=\sigma_{\omega 3}$	$\sigma_{scalefact}$	$\sigma_{scaledot}$	$\sigma_{scaleddot}$
	2.16	1.49	2.14	2.87	1.54	3.42	2.09E-06	1.95E-06	2.13E-06
	Correlation Matrix * 1								
	ε_1	ε_2	ε_3	ω_1	ω_2	ω_3	scalefact	scaledot	scaleddot
ε_1	1	0.11	0.06	-0.03	0	-0.09	-0.11	0	-0.01
ε_2		1	-0.28	-0.08	-0.07	-0.19	0.06	-0.24	0.19
ε_3			1	-0.10	-0.10	-0.05	0.09	0	0.02
ω_1				1	0.58	-0.12	0.14	-0.09	-0.46
ω_2					1	-0.36	0.02	0.02	-0.32
ω_3						1	-0.02	0.44	0
scalefact							1	0.10	-0.32
scaledot								1	-0.48
scaleddot									1
	1991.25 solution:								
	σ_γ $=\sigma_{\varepsilon 1}$	σ_β $=\sigma_{\varepsilon 2}$	σ_α $=\sigma_{\varepsilon 3}$	$\sigma_{\dot{\gamma}}$ $=\sigma_{\omega 1}$	$\sigma_{\dot{\beta}}$ $=\sigma_{\omega 2}$	$\sigma_{\dot{\alpha}}$ $=\sigma_{\omega 3}$	$\sigma_{scalefact}$	$\sigma_{scaledot}$	$\sigma_{scaleddot}$
	8.95	4.96	10.59	2.87	1.54	3.42	2.09E-06	1.95E-06	2.13E-06
	Correlation Matrix 1*								
	ε_1	ε_2	ε_3	ω_1	ω_2	ω_3	scalefact	scaledot	scaleddot
ε_1	1	0.55	-0.07	-0.97	-0.56	0.10	-0.17	0.09	0.44
ε_2		1	-0.27	-0.56	-0.95	0.28	0.00	-0.09	0.36
ε_3			1	0.10	0.33	-0.98	0.04	-0.42	0
ω_1				1	0.58	-0.12	0.14	-0.09	-0.46
ω_2					1	-0.36	0.02	0.02	-0.32
ω_3						1	-0.02	0.44	0
scalefact							1	0.10	-0.32
scaledot								1	-0.48
scaleddot									1

liminary *Hipparcos* data and *HST* data in 1993 (Lalich 1994). New solutions were performed as more *Hipparcos* and *HST* data became available.

To insure compatibility for the final system determination, the *Hipparcos* Project imposed two restrictions on the presentation of the final results from the various link techniques. The first restriction was that the presentation of the rotation matrix conform to the notation given in Lindegren & Kovalevsky (1995, op. cit.) and the second was that the errors of the observations be adjusted so that the χ^2 of the fit be equal to the number of degrees of freedom. In our case, the number of degrees of freedom was 69, and we found that adjusting the variances of the *HST* data, the *Hipparcos* proper motion data, and the *Hipparcos* parallax data had varying effects on the χ^2. In particular, for the "nominal" values of the variances assumed, the χ^2 was typically 4 or 5 times the number of degrees of freedom. We started by assuming that the VLBI variances contributed little to the χ^2, which was born out by the fact that increasing the variances on the VLBI positions did not significantly reduce the χ^2. We then assumed that the *HST* variances were underestimated. Increasing the *HST* variances led to a significant reduction of the χ^2, but not enough. We also noted that increasing the *HST* errors beyond a certain point (a factor of 6 or 8) did not reduce the χ^2 further. We then increased the variances on the *Hipparcos* proper motions, which effected a significant reduction of the fit χ^2, and increasing the variances on the *Hipparcos* parallaxes also effected a significant reduction. We experimented with various combinations of "variance enhancement." The final increases to the input variances were to multiply the *HST* input variances, and the *Hipparcos* proper motion and parallax variances each by 4. The resulting χ^2 was 72, compared to the 69 degrees of freedom. The largest difference in the rotation matrix elements between the unadjusted and adjusted solutions was 0.3 milliarcseconds in the rotational offset about the z axis. Therefore, adjustment of the formal variances had no significant affect on the final values of our link solution parameters.

In trying to normalize the χ^2 of the fit for the *Hipparcos* Project, we considered the χ^2 calculation itself. One can define a χ^2 parameter for each individual measurement: the square of the residual to the fit of that measurement divided

TABLE A1. Speckle results.

SAO #	N.R.	Diagnosis	Comments	INCA #	RA(1950) HHMMSS	Dec(1950) +/-ddmmss
74548	3	OK		5588		
109727	3	A				
74560	2	OK		5673		
109741	2	A				
109751	2	OK		5818		
147700	1	A				
109825	2	OK				
129297	2	A				
	1	A			12402	-002851
	1	A	2" pair		13304	324759
37354	2	OK				
37358	1	OK				
	1	OK		7587	13450	324634
	1	A			13453	325635
129448	1	OK				
	1	A	also has 5" component		14915	741108
74999	2	OK				
	1	OK		9131	15312	742251
	1	A			15538	742642
92782	2	A				
4613	1	OK				
12298	3	A	also has faint 5" comp.			
12301	2	OK				
12306	2	A				
75469	2	A	also faint 15" comp			
75488	2	A				
12419	2	A				
12425	1	A				
	1	OK		12845	24111	622253
12434	1	OK				
110894	2	A				
38715	2	OK				
	1	OK		15446	31552	410525
	1	A			31706	411132
	1	A	also 10" comp		40501	-121803
	1	OK		19278	40532	-121733
	1	OK		19290	40545	-121701
	1	OK			42200	2858
	2	A			42200	3747
	2	A			42253	2827
111881	2	OK				
	1	A			42958	52105
	1	OK			43037	52320
111893	3	OK		21272		
	2	OK			44700	842944
793	1	A				
804	2	OK				
112887	2	OK				
112889	3	OK	20" pr w/ 112890			
112890	1	OK	20" pr w/ 112889			
132447	2	A				
58576	2	OK	has a 3" comp			
58580	2	A				
132862	3	A				
151166	1	OK	marginal obs.			
986	1	A				
1002	1	A	also faint 10" comp			
59893	2	A				
59902	3	A				
6141	2	A	also very faint 10" comp.			
6152	3	A				
	2	OK		35542	71423	712618
	2	OK		35654	71546	711431
134649	1	OK				
97099	1	OK		37160		
97100	1	OK	faint 6" comp.			
97109	1	OK				
	1	OK	faint 20" comp		73608	15336
	1	OK			73623	20134
97213	1	OK				
135061	1	A				
135064	2	OK				
97219	2	OK				
42188	1	OK				
	1	OK		40935	81851	-124000
	1	A			81902	-123758
	1	OK			81941	-123726
42403	1	OK				
80229	2	A				
42421	1	OK				
26921	1	OK				
	1	OK			83257	710005
	1	A			83928	705921
	1	OK			84035	711459
80493	1	OK		43701		
154848	1	OK				
	1	A			91154	295041
	1	OK		45432	91234	300004
	1	A			91236	295554
	1	A			91254	294234
	1	OK			91424	293945
61482	1	OK				
61491	1	OK				
	1	A			95544	323730
	1	OK		48920	95550	324930
61792	1	OK		48952		
	1	OK			101933	310429
	1	OK		50796	101950	-101705
	1	OK			102009	310847
62008	1	OK				
	1	OK			103737	62752
	1	OK			103800	60917
	1	OK			103825	62204
118598	1	A				
62912	1	OK				
62943	1	A				
62945	1	A				
	1	OK			121926	284916
	2	OK			140426	284319
83172	2	OK				
	2	OK			140535	284656
120390	2	OK				
	2	OK			141700	63629
	2	OK			141723	64550
	2	A			141813	543303
29105	2	OK				
29110	2	OK				
16441	2	OK				
16446	2	A				
16453?	2	OK			143756	643022
16455	2	A				
101177	2	A				
101198	2	OK				
	2	A			145628	712639
	2	A			150018	713836
8140	2	OK				
	2	A	also 30"comp		150837	-53115
140370	2	OK				
140371	2	OK	20" pair with SAO 140372			
140373	2	OK				
	2	OK			150944	-90426
140401	2	A				
121210	5	OK				
121281	5	OK				
121283	5	OK				
65038	2	OK				
84214	2	A				
84223	2	A				
65401	5	OK				
65407	5	OK				
65424	5	OK				
30014	5	A				
	2	OK			163533	572657
65473	5	OK				
30044	2	OK				
	2	A	0	81828	164110	394316
	2	A	0		164157	400037
121960	4	A				
	2	OK			165525	45002
	2	A			165536	55137
	2	A			165609	50351
	2	A			165615	45354
102732	5	A				
102735	5	A				
65991	2	A				
65993	2	A				
	2	A			172125	343014
	2	A			172226	343700
122400	5	A	also 10" comp			
122404	5	A				
	2	OK			172557	501926
30405	2	OK				
30412	2	OK				
30415	2	A				
30419	2	A				
66142	2	A				
46881	2	OK				
141833	5	OK				
141841	5	OK				
	1	OK			174404	700529
8901	1	A				
122820	4	OK				
122838	4	OK				
	1	OK			174938	94123
47024	1	OK	ft 30" comp			
8937	1	A				
47038	1	OK				
47042	1	OK				
	1	A			180334	782637
	1	OK			180413	781953
	1	OK			180558	782801
	1	OK			182052	104215
	1	OK			182117	105507
	1	OK			182128	104050
103672	3	A				
103673	3	A				
103677	3	OK				
	1	A			182204	105038
	1	OK			182728	490027

TABLE A1. (continued)

SAO #	N.R.	Diagnosis	Comments	INCA #	RA(1950) HHMMSS	Dec(1950) +/-ddmmss
	1	A			182801	483930
	1	A	also ft 10" comp.		182818	484927
47545	2	OK				
	1	OK			182958	282311
86173	3	A				
86188	3	A				
	2	OK			192744	735938
	2	OK			192759	734731
9456	2	OK				
125096	2	OK				
125102	2	OK				
125107	2	A				
125116	2	OK				
9622	2	OK				
	2	OK			200707	775358
144138	1	A				
	2	OK			200827	780146
9657	2	OK				
9662	2	OK				
9665	2	A				
18812	2	A	also 10" comp			
18815	2	A	also 20" comp			
18836	2	OK				
32639	2	OK				
32741	2	OK				
32746	2	A	also 5" comp			
32758	2	OK				
32765	2	A				
89550	2	OK				
89564	2	OK				
	1	A			212729	-120518
	1	OK			212801	-120008
	2	A			212821	44411
164452	1	OK				
	1	OK		106347	212936	-121735
164461	1	OK				
145482	1	OK				
145490	1	OK				
145504	1	OK				
126915	1	OK	has 6" comp			
107307	1	OK				
127056	1	OK				
127062	1	OK				
127069	1	OK				
127070	1	A				
51545	1	OK				
	1	OK		108776	220002	420816
51584	1	OK		108795		
71982	1	A		108857		
	1	OK			220111	421926
	1	A			220121	314936
	1	OK			221527	-40401
	1	OK			221531	-40015
	1	OK			221540	-35704
146083	1	OK				
146122	1	OK				
90642	1	OK				
90650	1	OK				
	1	A			224329	-122629
165283	1	A				
	1	OK			224738	135901
	1	OK			224741	141011
108213	1	OK				
	1	OK			224905	140645
108232	1	OK				
	1	OK		113060	225119	160132
108243	1	OK		113115		
52500	1	OK				
	1	OK			225347	72816
	1	A			225348	72237
52518	1	OK				
127859	1	OK				
128124	1	Ok				
128126	1	OK				
	1	A			231816	270858
91194	1	OK				
	1	OK			231841	271620
91223	1	OK				
108657	1	OK				
91412	1	OK				
	1	OK			233742	262449
	1	OK	faint 10" comp.		233811	263604
128378	1	OK				
128381	1	A	2" pair !			
53471	1	A				
53473	1	OK				
53479	1	A				
53490	1	OK				

by the square of the expected error of that measurement. In the final selection of "good" observations, we sorted the observations by their χ^2 values, and plotted the values against their sorted number. An example is given in Fig. 10. Three observations with very large individual χ^2's were dropped from the final solution.

Upon receipt of the final *Hipparcos* data (H37 in 1996 January) we performed a new solution. We also included new *HST* data with revised calibrations in the solution. The rotation about the z axis from that solution differed from previous solutions by an unacceptably large (>10 mas/yr) amount. We undertook an intensive investigation to determine the cause of the discrepancy, including scrutinizing the software and all the calibrations. Ultimately, we used the technique of performing complete system solutions, but dropping one successive *HST* observation set from each solution. We performed 83 solutions with 82 data sets in each solution. One observation set was pulling the solution out of line by ten milliarcseconds per year. The reason for the sensitivity to this particular *HST* observation set is still unclear, but we suspect that it is a geometric projection affect with the target pair close to one of the poles of rotation of the system solution. Investigation into this pair is continuing.

5.4 Results

The result of our final *Hipparcos*-ICRS link is given in Table 4. The (α,β,γ) parameters in the solution are the small angle rotational offsets around the (z,y,x) coordinate axes respectively. The $(\dot{\alpha},\dot{\beta},\dot{\gamma})$ parameters are the time derivatives of (α,β,γ). The time varying scale of the FGS is also included. The parametrization of the scale comprises an expansion/compression factor to the nominal scale of the FGS, and coefficients of the first and second time derivatives of the scale (scalefact, scaledot, scaleddot). The values given for the angle parameters are the deviations of our solution from the final system solution adopted by the *Hipparcos* Project (Kovalevsky *et al.* 1997). We performed solutions at two separate epochs: the approximate mean epoch of the *Hipparcos* data (1991.25) and the approximate mean epoch of the *HST* observations (1994.25). The two solutions are equivalent when the covariances are taken into account in projecting the system offset from one specific epoch to another. Table 4 also gives the standard deviations of the parameters and the covariances between them. Our solution derived from the *HST* data alone was combined with other solutions from other techniques by the *Hipparcos* Project in the final system solution.

Note that the formal error of the rotational offset (the epsilons) for the *Hipparcos* mean epoch is substantially larger than for the *HST* mean epoch, while the rotation rate error (the omegas) is the same. This effect comes from the projection of the rotational offset backward in time from the *HST* epoch to the *Hipparcos* epoch. The result is that the rotational offset at the *Hipparcos* epoch includes the propagation of errors in the rotation rate for three years. The effect is directly analogous to the degradation in the errors of a star's position off the mean epoch of a catalogue due to errors in the proper motion of the star.

The *Hipparcos* Project initiated several programs to determine the relationship between the *Hipparcos* reference frame and the ICRS. These included radio VLBI, VLA, and MERLIN observations of RS CVn stars, photographic observations of stars with respect to EGOs, and the *HST* program described here. Other, pre-existing programs were also used to derive the frame rotation parameters: the Lick and Yale proper motion programs in the Northern and Southern hemispheres (NPM and SPM), and analysis of the earth-rotation parameters derived from ongoing measurements made over many years to determine universal time and the motion of the earth's pole. The final formal errors from the different techniques are 0.6 mas in the three axis components, and 0.25 mas/yr in the components of the time derivatives of those components.

6. CONCLUSIONS

Observations of separations of *Hipparcos* Stars from Extragalactic Objects have been made with the Fine Guidance Sensors of the *Hubble Space Telescope*. These observations have been used to determine the rotation of the *Hipparcos* Instrumental System with respect to the ICRS-VLBI reference frame. The determination from 78 observations yields accuracies on the order of 2 mas rms in the coordinate rotational offsets near the mean epoch of the *HST* observations and 2 mas/year in the coordinate rotation rates. The main contributing sources of error are the *HST* errors and the errors in the proper motions in the *Hipparcos* Catalogue projected over the time between the *Hipparcos* mean epoch (1991.25) and the *HST* mean epoch (1994.25).

Repeated separation measurements made on a single pair spanned at most two years, but in most cases spanned only one year. By repeating the separation measurement in the near future, with a time difference of 4 or more years, the solution for the time variable rotation will be improved by a factor of 4. Reduction of the guide star positions to the *Hipparcos*/Tycho system, plus a knowledge of the FGS to FGS alignment within the *HST* focal plane structure should allow us to determine right ascension and declination differences at the few milliarcsecond level from our existing and any new data. This new information would double the amount and usefulness of our data. Continuing improvement of knowledge of the FGS distortions will reduce the uncertainties. Because the whole *Hipparcos* reference system is estimated to be systematically good to a tenth of a mas or better, further observations are needed to reduce the errors in the system rotation and offset to the level of accuracy where the *Hipparcos* errors themselves dominate the uncertainty of the link.

This work is based on observations with the NASA/ESA *Hubble Space Telescope*, obtained at the Space Telescope Science Institute, which is operated by the Association of Universities for Research in Astronomy, Inc., under NASA Contract No. NAS5-26555. This work is also based on data from the *Hipparcos* astrometry satellite. We acknowledge support for the *Hubble Space Telescope* Astrometry Science Team, through NASA Grant No. NAG5-1063 and Contract No. NAS5-29285 which funded the development of the astrometric capabilities and the GTO portion of the *HST* data used herein. We acknowledge Grants No. NAGW233, NAGW1537, and NAGW3111 from NASA Headquarters for the direct support of this work since 1982, and we appreciate the foresight and commitment from NASA through all the trials and tribulations of both *HST* astrometry and *Hipparcos* to the successful conclusion of this project. We acknowledge the GO (under Grant No. GO-3819-01.91A from the Space Telescope Science Institute) and GTO (under the Astrometry Science Team support over the years) time that allowed us to make the significant numbers of *HST* observations necessary to complete this project. We are grateful to the U.K. Science and Engineering Research Council for the allocation of speckle observing time on the 3.9 m Anglo-Australian Telescope and for funding travel and support (Argue *et al.* 1984, 1985); also to Professor D. S. Matthewson for time on the Mt. Stromlo 1.9 m telescope. We are grateful to the Center for High Angular Resolution Astronomy under Professor Harold McAlister for including many of the northern hemisphere stars in their program. We thank the Space Telescope Science Institute for all of their help in obtaining and understanding the nature of the FGS astrometric data. We acknowledge the debt we owe to the personnel at the now Hughes Danbury Optical Systems Corporation who have been instrumental in designing and building the FGS with attention to the needs of Astrometry. We acknowledge with gratitude the contribution of the personnel of the *Hipparcos* project, and particularly the Input Catalogue Consortium for their work in analyzing all our target fields for potential *Hipparcos* problems: work critical to the final selection of our targets. In 1996, Jerry Kristian died in a tragic accident. During the course of this project he provided encouragement and insight that led to the choice of optimum targets given the constraints of the satellites. His quiet wisdom and gentle nature are missed sorely, and we dedicate this work to his memory.

APPENDIX: THE NORTHERN SPECKLE INTERFEROMETRY OBSERVATIONS OF CANDIDATE *HIPPARCOS* STARS

From 1982 until 1990, several hundred speckle observations were made of candidate *Hipparcos* stars. The northern hemisphere observations were made with the Georgia State University Speckle Camera in the swashbuckling days of speckle observations. The autocorrelations were performed in real time at the telescope, and the television screen was viewed to detect any obvious duplicity at the several arcsecond level. The "diagnosis" (see below) generally applies to the range of separation of 0.03 to 0.70 arcseconds. The range between 0.7 and 1.5 arcsec is mostly unsampled due to the size of the field examined by the correlator on one hand and the resolution of the television monitor on the other. In assessing nonsingularity, we were conservative in that many of the objects judged "to avoid" could be "spurious peak" objects that may yet be single. Table A1 lists the stars observed and the results. Column 1 gives the SAO number when available. Column 2 gives the number of reduced observations. Column 3 gives the "diagnosis": OK means no detected duplicity, "A" means avoid using as a target if possible; the speckle autocorrelation showed signs of nonsingularity. Column 4 gives the comments (made at the telescope, in most cases). Column 5 gives the Hipparcos Input Catalogue number. Column 6 gives the 1950 right ascension in hours, minutes and seconds of time. Column 7 gives the 1950 declination in degrees, minutes, and seconds, for the non-SAO stars.

REFERENCES

Argue, A. N., Hebden, J. C., Morgan, B. L., & Vine, H. A. 1984, MNRAS, 206, 669

Argue, A. N., Hebden, J. C., Morgan, B. L., Standley, C., & Vine, H. A. 1985, MNRAS, 216, 447

Benedict, G. F., *et al.* 1992, PASP, 104, 958

Benedict, G. F., *et al.* 1994, PASP, 106, 327

Bergeron, J. 1992, IAU Transactions, XXIB (Kluwer, Dordrecht), p. 41

Bozyan, E. P., Hemenway, P. D., & Argue, A. N. 1990, AJ, 99, 1421

Eichhorn, H. 1974, Astronomy of Star Positions (Frederick Ungar, New York), Section 3.2.2, 111ff

Hemenway, P. D., & Duncombe, R. L. 1986, in Astrometric Techniques, edited by H. K. Eichhorn and R. J. Leacock (IAU, Reidel, Dordrecht), p. 613

Jefferys, W. H., Fitzpatrick, M. J., & McArthur, B. E. 1988, Celest. Mech., 41, 39

Kovalevsky, J., *et al.* 1997, A&A, 323, 620

Lalich, A. 1994, Thesis, Master of Science in Engineering, The University of Texas at Austin

Lindegren, L., & Kovalevsky, J. 1995, A&A, 304, 189

Shattuck, F. E. 1992, Thesis, Master of Science in Engineering, The University of Texas at Austin

Whipple, A. L., *et al.* 1996, Post-servicing Mission Calibration Workshop, STScI 1995 May 15–17, Space Telescope Science Institute, Baltimore, p. 119

White, G. L., & Jauncey, D. L. 1988, in Fundamentals of Astrometry, edited by H. K. Eichhorn, C. A. Murray, and A. Upgren (IAU, Reidel, Dordrecht)